ACS OMEGA

http://pubs.acs.org/journal/acsodf

Article

Design, Synthesis, and Biological Activity of Donepezil: Aromatic Amine Hybrids as Anti-Alzheimerss Drugs

Dan Wan, Feng-Qin Wang, Jiang Xie, Lin Chen,* and Xian-Li Zhou*

Cite This: *ACS Omega* 2023, 8, 21802−21812

Read Online

ACCESS | Metrics & More | Article Recommendations | Supporting Information

ABSTRACT: In this study, benzylpiperidine, the active group of donepezil (DNP), was connected with the neurotransmitter phenylethylamine by square amide, in which the fat chain of phenylethylamine was reduced and the benzene rings were substituted. A series of multifunctional hybrid compounds, including DNP−aniline hybrids (**1**−**8**), DNP−benzylamine hybrids (**9**−**14**), and DNP−phenylethylamine hybrids (**15**−**21**) were obtained and their cholinesterase inhibitory activity and neuroprotection of the SH-SY5Y cell line were determined. Results showed that compound **3** exhibited excellent acetylcholinesterase inhibitory activity with an IC_{50} value of 4.4 μM, higher than that of positive control DNP and significant neuroprotective effects against H_2O_2-induced oxidative damage in SH-SY5Y cells with 80.11% viability rate at 12.5 μM, much higher than that of the model group (viability rate = 53.1%). The mechanism of action of compound **3** was elucidated by molecular docking, reactive oxygen species (ROS), and immunofluorescence analysis. The results suggest that compound **3** could be further explored as a lead compound for the treatment of Alzheimer's disease. In addition, molecular docking research indicated that the square amide group formed strong interactions with the target protein. Based on the above analysis, we believe that square amide could be an interesting construction unit in anti-AD agents.

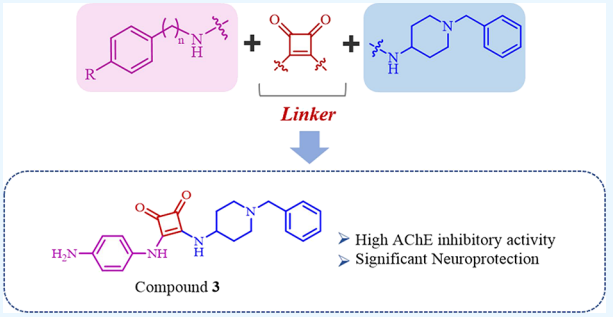

1. INTRODUCTION

Alzheimer's disease (AD) is a multifactorial neurodegenerative disease. Its clinical manifestations include loss of memory function, cognitive function, visual space function, and self-care ability.[1−3] The progression of AD is associated with loss of cholinergic transmission, oxidative damage, imbalance of metallics, excitotoxicity, and neuroinflammation, which can lead to a "domino" cascade of events in AD.[4−9] At this stage, the efficacy of most single drugs can only be based on delaying the course of the disease, and it is difficult to further prevent and block the course of the disease fundamentally and as a whole. Due to the complexity of AD disease, single-target drugs cannot provide an ideal therapeutic effect.[10] Therefore, there was potential significance in the study of multi-target anti-AD agents.

Molecular hybridization mainly combines the basic structure of two or more drugs in one molecule or pharmacophore groups of different drugs in one molecule to exert pharmacological activity or dual action. Since the 21st century, the application of molecular hybridization in the research and development of new drugs has become more and more common, has achieved good results, and has gradually become a breakthrough in new drug research and development.[11−13] Among them, the design concept of Benoxate is to hybridize aspirin with acetaminophen using molecular hybridization, which reduces the irritation of aspirin in the gastrointestinal tract and synergizes the effect.[14]

Donepezil (DNP) has been approved by the FDA for the treatment of Alzheimer's disease as the second generation of reversible specific central acetylcholinesterase (AChE) inhibitor.[15] N-benzylpiperidine in its structure is the primary pharmacophore responsible for AChE inhibition, which could inhibit the hydrolysis of acetylcholine, accumulate the release of acetylcholine released from cholinergic nerve fibers continuously, and excite choline receptors.[16,17] Phenylethylamine is a kind of monoamine neurotransmitter that plays an important role in neuroregulation by increasing the level of dopamine in extracellular fluid and inhibiting the activation of the dopamine nerve. Phenylethylamine has been widely used in the treatment of Parkinson's disease.[18] Since DNP and phenylethylamine have significant therapeutic activity in neurodegenerative diseases, combining hotspot drugs for PD with anti-AD drugs may provide a new avenue for the treatment of AD.

Barbora Svobodova's research group[19] first introduced a square amide group in the design of anti-Alzheimer's drugs in 2019, and its four-ring system can act as an ideal hydrogen bond donor or acceptor so that the group not only acts as a linker but its own hydrogen bond donor and acceptor groups can also

Received: March 3, 2023
Accepted: May 25, 2023
Published: June 5, 2023

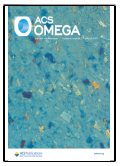

Scheme 1. Synthesis of DNP-Phenylethylamine Hybrids

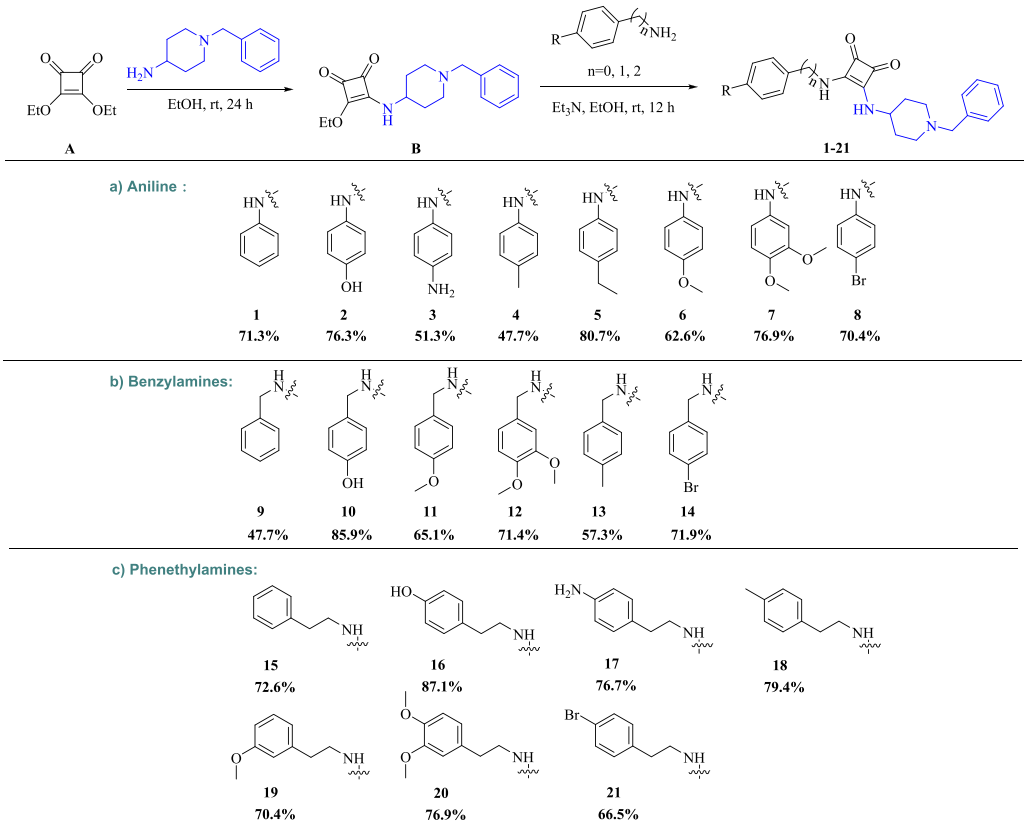

Table 1. Inhibitory Activity against AChE by Compounds 1−21

compound	AChE inhibition [%][a] 25 μmol/L	AChE inhibition [%][a] 12.5 μmol/L	compound	AChE inhibition [%][a] 25 μmol/L	AChE inhibition [%][a] 12.5 μmol/L
1	55.71 ± 1.56	48.82 ± 0.32	**12**	70.06 ± 1.34	60.94 ± 2.43
2	66.67 ± 2.35	53.45 ± 1.38	**13**	60.29 ± 0.65	45.21 ± 0.42
3	76.97 ± 0.44	68.86 ± 2.46	**14**	54.11 ± 2.52	42.92 ± 1.92
4	69.47 ± 1.36	55.59 ± 1.64	**15**	59.00 ± 1.47	45.45 ± 0.33
5	50.42 ± 0.54	43.18 ± 0.54	**16**	63.85 ± 0.71	48.30 ± 0.38
6	64.48 ± 1.25	58.96 ± 0.76	**17**	69.46 ± 1.43	60.14 ± 2.22
7	62.42 ± 2.34	49.57 ± 1.74	**18**	52.17 ± 1.54	43.85 ± 1.34
8	42.90 ± 0.34	40.36 ± 0.48	**19**	54.61 ± 0.32	45.68 ± 0.55
9	51.63 ± 1.39	38.67 ± 2.54	**20**	59.33 ± 2.12	50.93 ± 1.27
10	54.86 ± 2.65	42.03 ± 0.79	**21**	45.65 ± 1.40	30.06 ± 1.32
11	65.89 ± 1.34	60.97 ± 0.53	**DNP**	75.38 ± 0.47	64.22 ± 1.59

[a]AChE from *Electrophorus electricus* was used, and percent inhibition data are the mean ± SD of three independent experiments performed in duplicate.

interact with complementary sites in a variety of ways.[20] Given the great potential for the application of square amide groups in the design of Alzheimer's disease drugs, we use square amide as a bridge to connect to link the N-benzylpiperidine in DNP with phenylethylamine to design DNP-square amide-phenylethylamine derivatives, with aliphatic chain reduction of the phenylethylamine portion and various substitutions on the benzene ring, resulting in DNP−benzylamine hybrids, and DNP−aniline hybrids. Subsequently, the cholinesterase inhibitory activity, SH-SY5Y cytotoxicity, and neuroprotective effects against H_2O_2-induced oxidative damage in cells of the prepared compounds were determined.

2. RESULTS AND DISCUSSION

2.1. Chemistry. The synthesis of DNP-phenylethylamine heterozygous derivatives is described (Scheme 1.) All the compounds were synthesized according to the previously reported method.[21] The types of bases are discussed, as well as sodium ethoxide, sodium hydride, and triethylamine. As an organic base of the system, the results show that when triethylamine is added to the reaction system as an acidic binder, the reaction can be carried out more efficiently, and when the reaction time is controlled at about 10 h, the yield is improved. In general, the Michael addition reaction of 4-amino-1-benzylpiperidine with diethyl squarate was carried out to obtain the intermediate **B**. Then, the phenylethylamine portion was subjected to aliphatic chain curtailment and various

https://doi.org/10.1021/acsomega.3c01427
ACS Omega 2023, 8, 21802−21812

substitutions on the benzene ring, and the amino part subsequently further reacted with another ethoxy in diethyl squarate to prepare the target compound. Three series of derivatives, namely aniline (**1**−**8**), benzylamine (**9**−**14**), and phenylethylamine (**15**−**21**), were designed and synthesized. According to the method described in the reference, an array of aniline with diversely substituted aryl groups reacted smoothly with intermediate **B** in the presence of triethylamine, providing corresponding products **1**−**8** with moderate to good yield. On the other hand, moderate to outstanding yields were generally attained for benzylamines with diversely substituted aryl groups (products **9**−**14**). Moreover, phenethylamines with diversely substituted aryl groups were also applicable to produce products **15**−**21** in excellent yields. All the structures of target products were determined according to their nuclear magnetic resonance spectrum analysis and liquid chromatography mass spectrometer.

2.2. Biological Activities. *2.2.1. Evaluation of ChE Inhibitory Activity.* The determination of the inhibitory capacity of a drug on AChE is an important aspect when designing drugs for AD treatment. By measuring the inhibitory activity of a drug against AChE, the utilization of ACh in cholinergic synapses can be further evaluated. On this basis, we assessed the inhibitory activity of compounds for the AChE using the Ellman method.[22] Overall, the results showed that there were many synthetic derivatives that exhibited moderate or excellent AChE inhibitory activity at 25 μM (Table 1).

(1) In the series of DNP−aniline hybrids, we observed that when there was no substituent at the aniline para-position (compound 1), it achieved 55.71% acetylcholinesterase inhibition at 25 μM. The cholinesterase inhibition rate was significantly enhanced when the aniline para-position was attached to an electron donor group compared to compound **1**. Compound **3**, which had an amino group attached to the aniline para-position, showed the most significant bioactivity (AChE inhibition = 76.97%) than the positive drug DNP at 25 μM, followed by compounds **2** and **4**, with an inhibition rate of 66.67 and 69.47%, respectively. The structural difference between compound **3** and compound **2** lies in the difference in substituents. The nitrogen atom of the primary amine in compound **3** has a lone pair of electrons, which is conjugated to the benzene ring and has a strong electron-giving ability. However, the hydroxyl group in compound **2** is not as strong an electron donor as the amino group, and its inhibitory activity is reduced. In contrast, when the electron-absorbing group bromine atom was attached to the aniline para-position, as in compound **8** (AChE inhibition = 42.90%), its biological activity was significantly reduced.

(2) In the series of DNP−benzylamine hybrids, we observed that the acetylcholinesterase inhibition rate could reach 51.63% when benzylamine had no substituent at the para position (compound **9**). In contrast, the acetylcholinesterase inhibition rate was 65.89 and 70.06% when the benzylamine was attached to the electron-donating group methoxy at the para-position (compound **11** and compound **12**). When the electron-absorbing group bromine atom was attached to the benzylamine para-position, as in compound **14** (AChE inhibition = 54.11%), its biological activity was significantly reduced.

(3) In the series of DNP−phenylethylamine hybrids, we observed that when there was no substituent at the phenylethylamine para-position (compound **15**), it exhibited 59.00% acetylcholinesterase inhibition. In contrast, when the phenylethylamine para-position was attached to the electron-donating groups hydroxyl and amino in turn (compound **16** and compound **17**), its cholinesterase inhibitory activity showed a slight increase relative to compound **15**, with acetylcholinesterase inhibition rates of 63.85 and 69.46%. In contrast, when the electron-absorbing group bromine atom was attached to the para-position of phenylethylamine, as in compound **21** (AChE inhibition = 45.65%), its biological activity decreased significantly.

From the above activity data analysis, it can be concluded that the acetylcholinesterase inhibitory activity of the DNP−aniline hybrids was superior to that of the benzylamine and phenylethylamine DNP hybrids. The analysis of the bioactivity data showed that the introduction of amino, hydroxyl, and methoxy groups enhanced the bioactivity, whereas the introduction of bromine atoms reduced it. Among them, compound **3** showed higher inhibition of acetylcholinesterase at 25 μM than the positive drug DNP.

The derivatives with excellent anti-AChE effect at 25 μM were assayed at a half maximum inhibitory concentration (IC_{50}). As shown in Table 2, compound **3** had the best acetylcholinesterase inhibitory activity (IC_{50} = 4.4 μM), which was higher than the positive control DNP (IC_{50} = 4.7 μM). Compounds **12** (IC_{50} = 5.6 μM) and **17** (IC_{50} = 6.9 μM) showed a comparable inhibitory capacity to the positive control.

Table 2. IC_{50} Values of Selected Compounds against AChE[a]

compound	$IC_{50} \pm SD$ (μM)[b]
2	9.6 ± 1.5
3	4.4 ± 1.7
4	8.3 ± 1.2
11	7.0 ± 0.5
12	5.6 ± 1.9
17	6.9 ± 0.4
DNP	4.7 ± 0.7

[a]AChE from electric eel was used. [b]Data are the means ± SD of at least three determinations.

2.2.2. Molecular Docking Study of Selected Compounds with AChE. Molecular docking is a useful tool for complex interactions between the receptor and the ligand. To further investigate the binding ability and mode of selected compounds with AChE, molecular modeling was carried out.

Due to the significant acetylcholinesterase inhibitory activity of compound **3**, we present the interaction pattern of compound **3** with the amino acid residues of AChE (PDB:4EY7),[23] as shown in Figure 1.

The docking results showed that compound **3** docked to the central gap region of the AChE protein and formed an intense interaction with AChE through the formation of hydrogen bonds and hydrophobic interactions with nearby amino acid residues. The central docking active site is the cavity composed of amino acid residues such as TRP86, TYR337, PHE338, TYR341, ASP74, TYR72, and TYR124. Analysis of the interactions showed that the nitrogen atom on the piperidine ring of benzyl piperidine forms π−cationic interactions with amino acid residues TYR337, ASP74, and PHE338. The

https://doi.org/10.1021/acsomega.3c01427
ACS Omega 2023, 8, 21802−21812

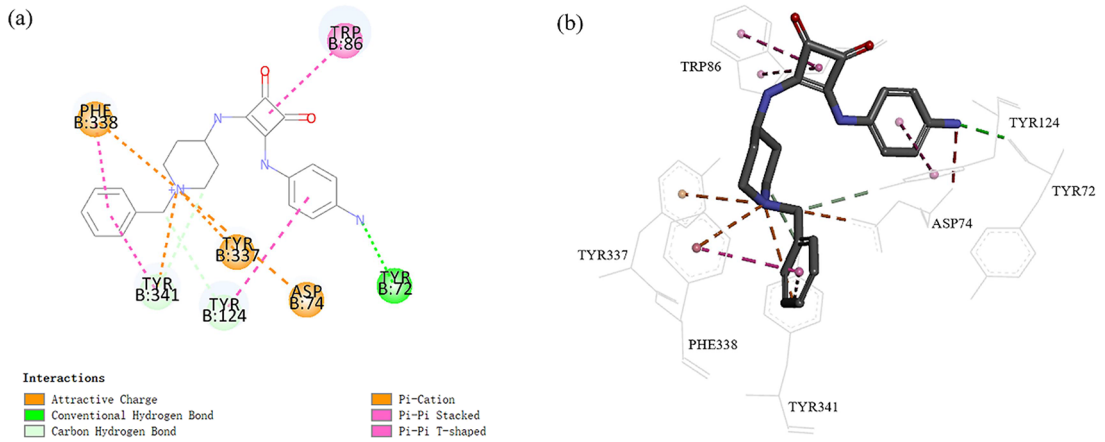

Figure 1. (a) Optimal pose of compound **3** at the active site of AChE (b) residues of the active site involved in ligand binding. PDB:4EY7.

benzene ring of benzyl piperidine forms a π−cation interaction with TYR341 and the amino group in the aniline ring forms a hydrogen bond with TYR72. The carbonyl group in the square amide forms van der Waals interactions with GLY121, whose double bonds form π−π stacked with TRP86.

We further predicted the binding site of compound **8** to AChE because of its lowest acetylcholinesterase inhibitory activity. The difference in the aniline para group in the structures of compound **3** and compound **8** resulted in a large difference in activity, where the aniline para group of compound **8** was attached to a bromine atom which, by molecular docking analysis, formed an unfavorable interaction with PRO88, resulting in a reduced binding capacity for AChE. (Figure S6).

The binding sites of other selected compounds with AChE were predicted. The molecular docking results showed compounds **2**, **4**, **11**, **12**, and **17**, also accommodated well in AChE with the energy of −18.7, −19.2, −19.6, −19.9, and −19.7 kcal/mol (Table 3). The highest-scored poses of the ligands are depicted in Supporting Information Figures S1−S5.

Table 3. Interaction Energy of Selected Compounds Docked with AChE

compound	interaction energy (kcal/mol)
2	−18.7
3	−20.2
4	−19.2
11	−19.6
12	−19.9
17	−19.7
DNP	−20.1

As shown by the interaction energy, compound **3** was the compound with the lowest interaction energy, indicating that it bound most strongly to AChE. Compound **12** had slightly higher interaction energy than compound **3**. Compound **2** had the highest interaction energy compared to the other selected compounds, indicating that it was less able to bind AChE.

Molecular docking showed that compound **3** has a strong interaction with AChE as well as a low binding energy, and from this perspective, we further verified that compound **3** has excellent acetylcholinesterase inhibitory activity.

2.2.3. Neuroprotective Effects against H_2O_2-Induced Oxidative Damage in Cells. Safety is extraordinarily important for central nervous system drugs, so the MTT method[24] was used to determine the toxicity of the synthesized compound in neuron cell line SH-SY5Y. As shown in Table 4, most compounds showed low toxicity to SH-SY5Y cells at 12.5 and 6.25 μmol/L.

Protection of neuronal cells from damage is an effective way to slow or prevent the progression of AD. Therefore, the neuroprotective activity of compounds against H_2O_2-induced oxidative damage in cells was evaluated by MTT assays. Then, the compounds with low toxicity to SH-SY5Y cells were selected to study further the neuroprotective effects of these compounds on H_2O_2-induced oxidative cells.

As shown in Table 5, compared with DNP, most compounds showed neuroprotective effects on H_2O_2-induced oxidative damage in cells from the analysis of bioactivity data:

(1) In the series of DNP−aniline hybrids, we observed that when there was no substituent attached to the aniline para position (compound **1**), the cell survival rate could reach 62.64%. The neuroprotective activity was significantly enhanced when the aniline para-position was attached to an electron-giving group compared to compound **1**. Compound **3** showed the most significant biological activity (survival rate = 80.11%) with the amino group attached to the aniline para-position, while compounds **2**, **4**, and **6** showed better biological activity with cell survival rates of 70.21, 68.16, and 60.63%, respectively. In contrast, when the electron-absorbing group bromine atom was attached to the para-position of aniline, as in compound **8** (survival rate = 50.46%), the biological activity was significantly reduced.

(2) In the series of DNP−benzylamine hybrids, we observed that cell survival rates of 57.44% were achieved when there was no substituent at the benzylamine para-position (compound **9**). The neuroprotective activity was slightly increased compared to compound **9** when the hydroxyl and methyl groups were attached to the benzylamine para-position in sequence, as in compound **10** and compound **13**, with cell survival rates of 59.59 and 58.87%, respectively. Notably, in this series, compounds **11** and **12** were both attached to methoxy, but their biological activity was slightly lower than that of compound **9** without the substituent, with cell survival rates of only 54.57 and 55.72%.

(3) In the series of DNP−phenylethylamine hybrids, we observed that when there was no substituent at the phenylethylamine para-position (compound **15**), the cell

https://doi.org/10.1021/acsomega.3c01427
ACS Omega 2023, 8, 21802−21812

Table 4. Toxicity of Compounds 1−21 on SH-SY5Y Cells

compound	survival rate (%)[a] 12.5 μmol/L	6.25 μmol/L	compound	survival rate (%)[a] 12.5 μmol/L	6.25 μmol/L
1	117.14 ± 0.46	124.30 ± 0.49	**12**	102.01 ± 0.97	105.60 ± 0.67
2	101.89 ± 1.32	102.39 ± 1.49	**13**	95.67 ± 1.64	101.54 ± 1.74
3	102.86 ± 2.34	104.07 ± 0.52	**14**	84.74 ± 0.63	91.95 ± 0.52
4	94.83 ± 0.43	99.85 ± 1.43	**15**	118.01 ± 2.16	120.69 ± 1.55
5	67.61 ± 2.11	88.08 ± 2.02	**16**	87.29 ± 1.99	97.85 ± 0.46
6	101.97 ± 1.57	103.25 ± 0.48	**17**	96.36 ± 0.14	101.80 ± 2.78
7	79.33 ± 2.57	76.36 ± 1.98	**18**	101.34 ± 2.64	107.83 ± 0.69
8	96.09 ± 0.57	101.08 ± 1.44	**19**	77.87 ± 0.55	90.60 ± 2.06
9	113.66 ± 1.64	123.57 ± 0.43	**20**	98.34 ± 1.58	107.57 ± 1.38
10	97.82 ± 2.14	102.67 ± 2.01	**21**	91.45 ± 0.65	107.26 ± 0.59
11	100.63 ± 0.73	101.47 ± 1.79	**DNP**	95.21 ± 1.68	96.14 ± 0.12

[a]Data are expressed as means ± SD of three independent experiments.

Table 5. Neuroprotective Effects against H_2O_2-Induced Cell Death in SH-SY5Y Cells

compound	survival rate (%)[a] 12.5 μmol/L	compound	survival rate (%)[a] 12.5 μmol/L
1	62.64 ± 1.32	**12**	55.72 ± 0.64
2	70.21 ± 1.22	**13**	58.87 ± 1.48
3	80.11 ± 0.32	**15**	58.11 ± 0.26
4	68.16 ± 1.56	**17**	60.28 ± 0.55
6	60.63 ± 0.23	**18**	58.72 ± 1.38
8	50.46 ± 0.43	**20**	57.87 ± 0.26
9	57.44 ± 1.63	**21**	46.05 ± 1.59
10	59.59 ± 0.65	**DNP**	57.21 ± 0.54
11	54.57 ± 1.23		

[a]Data are expressed as means ± SD of three independent experiments.

survival rate could reach 58.11%. The neuroprotective activity also showed a slight increase relative to compound **15** when the phenylethylamine para-position was attached to the electron-donating groups amino and methyl (compound **17** and compound **18**), with cell survival rates of 60.28 and 58.72% in that order. Similarly, in this series of compounds, compound **20** was attached to methoxy, but its biological activity was slightly lower than that of compound **15** without substituents, with a cell survival of 57.87%, and the presence of methoxy had no significant effect on this biological activity.

From the above conformational analysis, it can be concluded that the neuroprotective activity of aniline−DNP hybrids was better than benzylamines and phenylethylamine DNP hybrids. By analysis of the bioactivity data, the carbon chain interval had a particular effect on the neuroprotective activity. When the aliphatic chain is at its shortest, the aniline nitrogen atom not only forms a p−π conjugation with the benzene ring but also forms a p−π conjugation with the square acid system, leaving the system in a highly conjugated state, which appears to enhance its neuroprotective activity. In addition, the entry of amino, hydroxyl, and methyl groups enhances the biological activity, and the entry of methoxy has no significant effect on this biological activity, while the entry of bromine atoms reduces the biological activity.

Next, we further investigated in detail the neuroprotective effects of compounds **2**, **3**, and **4**, which have excellent

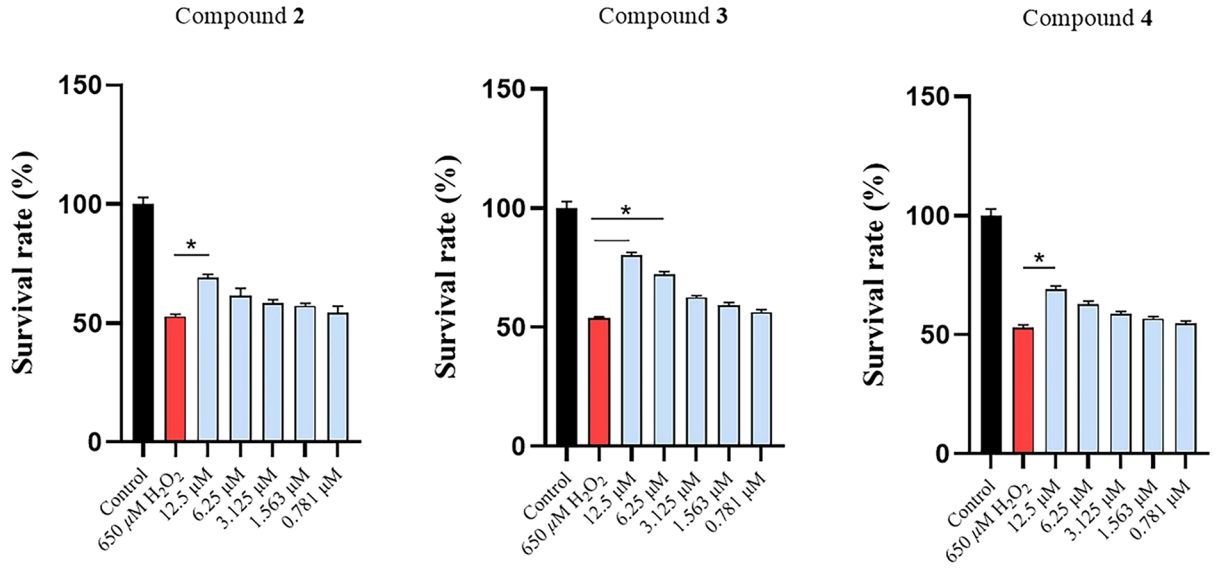

Figure 2. Protective activity of compounds **2**, **3**, and **4** against H_2O_2-induced neuronal cell damage. All data were representative of at least three independent experiments. *$p < 0.1$, **$p < 0.01$, and ***$p < 0.001$, vs H_2O_2-treated group.

https://doi.org/10.1021/acsomega.3c01427
ACS Omega 2023, 8, 21802−21812

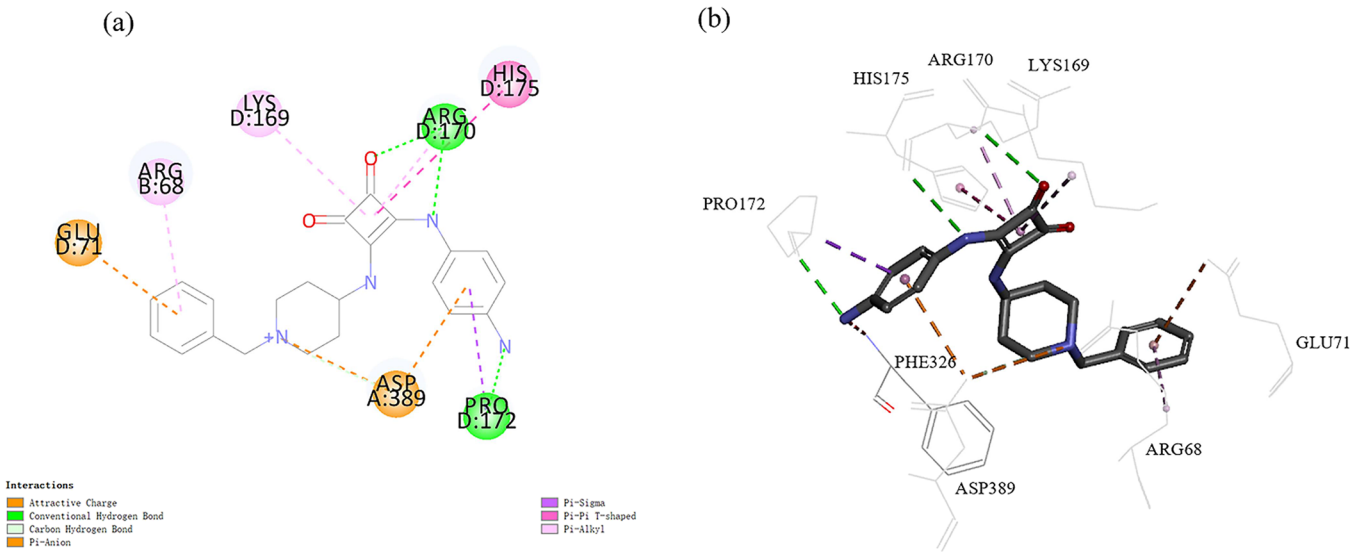

Figure 3. (a) Optimal pose of compound **3** at the active site of catalase (b) residues of the active site involved in ligand binding. PDB:1DGH.

neuroprotective activity, on H_2O_2-induced SH-SY5Y cells at different concentrations (12.5, 6.25, 3.125, 1.563, 0.781 μM). As shown in Figure 2, all the selected compounds showed neuroprotective effects in the concentration range and concentration-dependent neuroprotective activity at low concentrations. Of these, compound **3** showed the most significant neuroprotective activity, with a cell survival rate of 80.11% at 12.5 μmol/L.

2.2.4. Molecular Docking Study of Compound 3 with Catalase. Predicting possible interactions of compound **3** with catalase (PDB:1DGH)[25] involved in oxidative stress-related pathways using molecular docking analysis (Figure 3).

The docking results showed that compound **3** docked to the central void region of the catalase protein and formed a strong interaction with catalase by forming hydrogen bonds and hydrophobic interactions with nearby amino acid residues. The central docking active site is a cavity consisting of amino acid residues GLU71, ARG68, LYS169, ASP389, PRO172, ARG170, and HIS175. Analysis of the interactions shows that the nitrogen atoms on the benzyl piperidine ring form π−cationic interactions with the amino acid residues ASP389. The benzene ring of benzyl piperidine forms π−cationic interactions with GLU71, and the amino group on the aniline ring forms a hydrogen bond with PRO172. The carbonyl group in the square amide forms a hydrogen bond with ARG170, and the amino group in the square amide forms a hydrogen bond with ARG170.

2.2.5. Prediction of Compound 3's Pharmacokinetics Properties. Prediction by lipophilicity, water solubility, pharmacokinetics, and drug affinity presentation of compound **3** by the "pkCSM-pharmacokinetics" online platform (Table S1). Overall, absorption predictions indicate that compound **3** would be greatly absorbed by intestinal cells but not by the skin, which is desired since the compound is not meant to be dermally administered.

The five principles of pharmacophore determination show that compound **3** is a promising compound with good oral absorption and high bioavailability (Bioavailability Score: 0.55).

In addition, the water solubility of compound **3** with Log S (ESOL) = −3.93, soluble; Log S(Ali) = −4.42, moderately soluble; Log S(SILICOS-IT) = −6.36, insoluble. The predictions show that the water solubility of compound **3** is average. In subsequent experiments, we will further improve the aqueous solubility of compound **3**.

2.2.6. Mechanism of Neuroprotective Activity of Compound 3. H_2O_2 causes a decrease in mitochondrial membrane potential by activating oxidative stress, leading to apoptosis of nerve cells, and resulting in brain cell loss, while damage to apoptosis is thought to be mediated by ROS.[26] Because compound **3** has excellent acetylcholinesterase inhibitory activity and significant neuroprotective activity, the neuroprotective activity mechanism of compound **3** was further studied to explore whether compound **3** can inhibit intracellular apoptosis in nerve cells caused by ROS accumulation.

As shown in Figure 4A, the results indicate a dramatic increase in ROS production in the H_2O_2-treated cells relative to the control group. A significant reduction in intracellular ROS levels was observed in cells treated with compound **3** compared to model cells. The results suggest that compound **3** can inhibit H_2O_2-induced apoptosis by suppressing intracellular ROS accumulation.

By Tunel staining (Figure 4B), there was a large number of apoptosis in the H_2O_2 group, while compound **3** showed a significant ability to reverse apoptosis. This suggests that compound **3** can reduce the number of ROS in cells, thereby inhibiting H_2O_2-induced apoptosis.

2.2.7. Evaluation of the Complexing Ability of Metal Ions. Metal ions such as Cu^{2+}, Zn^{2+}, Fe^{2+}, and Al^{3+} contribute to the production of ROS, promote oxidative stress, and damage nerve cells.[27] Therefore, adjusting the concentration of metal ions is beneficial for the treatment of AD. The results of the above experiments showed that compound **3** exhibited significant neuroprotective and excellent acetylcholinesterase inhibitory activity. We further explored its metal-chelating ability to discover drugs possessing multiple activities. We used UV−vis spectroscopy[28] to evaluate the metal chelating ability of compound **3** (Figure 5). UV spectroscopy was used to study the chelating ability of biological metals such as Cu^{2+}, Zn^{2+}, Fe^{2+}, and Al^{3+}. The results showed that the UV absorption intensity of compound **3** changed significantly when aluminum, copper, iron, and zinc ions were added to the solution. The variation in

https://doi.org/10.1021/acsomega.3c01427
ACS Omega 2023, 8, 21802−21812

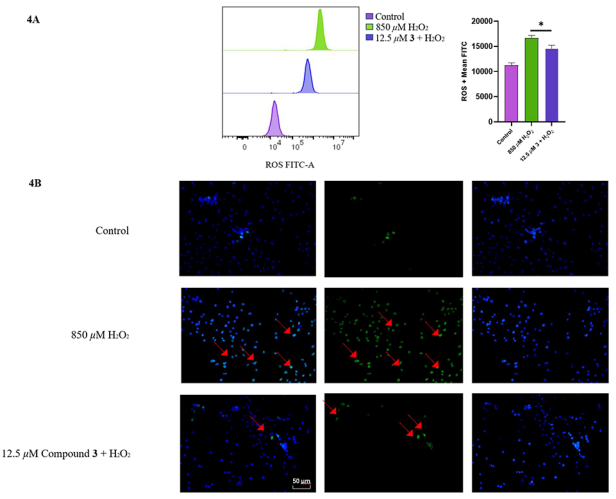

Figure 4. Compound **3** inhibits the production of ROS and protects against H_2O_2-induced apoptosis in SH-SY5Y cells. (A) SH-SY5Y cells were pretreated with 12.5 μM of compound **3** for 24 h, followed by treatment with 850 μM H_2O_2 for 4 h. ROS levels in SH-SY5Y cells were then measured by flow cytometry. Representative images and quantification of mean ROS FITC are shown. (B) SH-SY5Y cells were treated with H_2O_2 and compound **3**, stained with Tunel, and then observed with fluorescence microscopy. Scale bar: 50 μm. Apoptotic cells are indicated by red arrows.

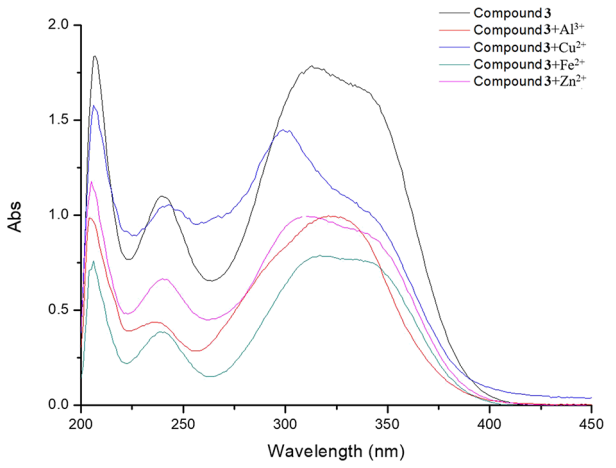

Figure 5. UV spectra of compound **3** (35 μM in methanol) alone and in the presence of $CuCl_2$, $ZnCl_2$, FeSO4, or $AlCl_3$ (35 μM in methanol).

the intensity of the samples confirms the existence of some interaction between compound **3** and the metal ions.

3. CONCLUSIONS

In summary, we used square amides as a bridge to connect N-benzyl piperidine with phenylethylamine compounds, by shortening the aliphatic chain of phenylethylamine and thus obtaining DNP−phenylethylamine hybrids, DNP-benzylamine hybrids, and DNP-aniline hybrids. The biological evaluation showed that compound **3** has excellent acetylcholinesterase inhibitory activity and prominent neuroprotective. The mechanism of action of compound **3** was elucidated by molecular docking, reactive oxygen species (ROS), and immunofluorescence analysis. Compound **3** was shown to inhibit H_2O_2-induced apoptosis by inhibiting the accumulation of intracellular ROS. The results suggest that compound **3** could be further explored as a lead compound for the treatment of Alzheimer's disease. In addition, molecular docking research indicated that the square amide group formed strong interactions with the target protein. Based on the above analysis, we believe that square amide could be an interesting construction unit in anti-AD agents.

4. EXPERIMENTAL SECTION

4.1. Chemical Synthesis. A solution of 3, 4-diethoxycyclobut-3-ene-1,2-dione (200 mg, 1.17 mmol, 1.0 equiv) and Et_3N (1.41 mmol, 1.2 equiv) in 5 mL of EtOH is cooled to 0 °C. Then, 4-amino-1-benzyl piperidine (1.17 mmol, 1.0 equiv) to the reaction mixture was added. The reaction mixture was stirred at room temperature for 24 h. The solvent was removed under reduced pressure. The crude product was purified by column chromatography (30 *g* of silica gel, eluent: dichloromethane/methanol = 15:1) to afford the intermediate **B**. A solution of **B** (200 mg, 0.64 mmol, 1.0 equiv) and Et_3N (0.76 mmol, 1.2 equiv) in 5 mL of EtOH is cooled to 0 °C. Then, the corresponding aniline (0.76 mmol, 1.2 equiv) is added to the reaction mixture. The reaction mixture is stirred at room temperature for 24 h. The solvent is removed under reduced pressure. The crude product is purified by column chromatography (30 g silica gel, eluent: dichloromethane/methanol = 15:1) to afford the target products.

Compound 1. White powder, yield: 71.3%. ^{1}H NMR (400 MHz, $CDCl_3$:DMSO-d_6 = 1:1) δ: 9.80 (s, 1H), 7.96 (s, 1H), 7.77 (d, J = 8.0 Hz, 2H), 7.63 (s, 2H), 7.63−7.62 (m, 2H), 7.61 (s, 1H), 7.59 (s, 1H), 7.56 (s, 1H), 7.31−7.25 (m, 1H), 4.36−4.26 (m, 1H), 3.88 (s, 2H), 3.19 (d, J = 11.0 Hz, 2H), 2.60−2.50 (m, 2H), 2.33 (dd, J = 12.8, 4.2 Hz, 2H), 2.01−1.89 (m, 2H). ^{13}C NMR (100 MHz, $CDCl_3$: DMSO-d_6 = 1:1) δ: 183.3, 180.0, 168.1, 163.6, 138.7, 128.9, 128.8, 128.6, 127.8, 126.7, 122.2, 117.7, 62.0, 51.0, 50.7, 32.8. HRESIMS m/z 362.1879 $[M + H]^+$ (calcd for $C_{22}H_{24}N_3O_2$, 362.1869).

Compound 2. White powder, yield: 76.3%. ^{1}H NMR (400 MHz, $CDCl_3$: DMSO-d_6 = 1:1) δ: 9.23 (s, 1H), 9.03 (s, 1H), 8.00 (s, 4H), 7.29 (d, J = 4.4 Hz, 1H), 7.24−7.17 (m, 3H), 6.73 (d, J = 8.8 Hz, 2H), 3.93 (s, 1H), 3.49 (s, 2H), 2.81 (d, J = 11.0 Hz, 2H), 2.19−2.05 (m, 2H), 1.98 (d, J = 9.8 Hz, 2H), 1.58 (q, J = 10.8 Hz, 2H). ^{13}C NMR (100 MHz, $CDCl_3$: DMSO-d_6 = 1:1) δ: 182.6, 180.2, 167.6, 163.7, 153.2, 137.9, 130.5, 128.5, 127.7, 126.5, 119.4, 115.5, 62.2, 51.1, 50.8, 33.0. HRESIMS m/z 378.1815 $[M + H]^+$ (calcd for $C_{22}H_{24}N_3O_3$, 378.1818).

Compound 3. White powder, yield: 51.3%. ^{1}H NMR(400 MHz, DMSO-d_6) δ: 9.31 (s, 1H), 7.53 (s, 1H), 7.34−7.26 (m, 4H), 7.23−7.20 (m, 1H), 7.08 (d, J = 8.2 Hz, 2H), 6.57−6.45 (m, 2H), 4.94 (s, 2H), 3.90−3.75 (m, 1H), 3.47 (s, 2H), 2.75 (d, J = 11.2 Hz, 2H), 2.09 (t, J = 11.2 Hz, 2H), 1.95−1.83 (m, 2H), 1.61−1.47 (m, 2H). ^{13}C NMR (100 MHz, DMSO-d_6) δ: 182.4, 180.4, 167.7, 163.8, 144.9, 138.2, 128.9, 128.2, 128.1, 127.0, 119.7, 114.3, 61.9, 51.1, 50.7, 32.8. HRESIMS m/z 377.1978 $[M + H]^+$ (calcd for $C_{22}H_{25}N_4O_2$, 377.1978).

Compound 4. White powder, yield: 47.7%. ^{1}H NMR (400 MHz, $CDCl_3$: DMSO-d_6 = 1:1) δ: 6.53−6.45 (m, 6H), 6.43−6.39 (m, 1H), 6.28 (d, J = 8.2 Hz, 2H), 2.67 (s, 2H), 1.99 (d, J = 12.4 Hz, 2H), 1.73−1.71 (m, 1H), 1.46 (s, 3H), 1.35−1.28 (m, 2H), 1.16 (d, J = 9.4 Hz, 2H), 0.85−0.66 (m, 2H). ^{13}C NMR (100 MHz, $CDCl_3$: DMSO-d_6 = 1:1) δ: 183.1, 180.0, 167.9, 163.5, 138.0, 136.2, 131.5, 129.4, 128.5, 127.8, 126.5, 117.7, 62.1, 51.1, 50.7, 33.0, 20.2. HRESIMS m/z 376.2023 $[M + H]^+$ (calcd for $C_{25}H_{30}N_3O_3$, 376.2025).

Compound 5. White powder, yield: 80.7%. ^{1}H NMR (400 MHz, $CDCl_3$: TFA-d = 10:1) δ: 7.94−7.92 (m, 3H), 7.94 (d, J =

https://doi.org/10.1021/acsomega.3c01427
ACS Omega 2023, 8, 21802−21812

14.4, 7.2 Hz, 2H), 7.65 (d, J = 7.8 Hz, 2H), 7.55 (s, 2H), 4.95−4.85 (m, 1H), 4.72 (s, 2H), 4.09 (d, J = 12.4 Hz, 2H), 3.53 (d, J = 13.6 Hz, 2H), 3.07 (q, J = 7.6 Hz, 2H), 2.81−2.64 (m, 4H), 1.65 (t, J = 7.6 Hz, 3H). ^{13}C NMR (100 MHz, $CDCl_3$: TFA-d = 10:1) δ: 183.3, 170.1, 167.4, 134.2, 133.7, 133.4, 132.9, 132.2, 130.0, 129.9, 124.1, 64.9, 54.8, 52.5, 32.8, 31.2, 18.1. HRESIMS m/z 390.2203 $[M + H]^+$ (calcd for $C_{24}H_{28}N_3O_2$, 390.2182).

Compound 6. White powder, yield: 62.6%. ^{1}H NMR (400 MHz, $CDCl_3$: DMSO-d_6 = 1:1) δ: 9.32 (s, 1H), 7.31−7.26 (m, 7H), 6.87−6.82 (m, 2H), 3.91 (s, 1H), 3.74 (s, 3H), 3.48 (s, 2H), 2.80 (d, J = 11.2 Hz, 2H), 2.19−2.08 (m, 2H), 2.03−1.91 (m, 2H), 1.57 (d, J = 12.0 Hz, 2H). ^{13}C NMR (100 MHz, $CDCl_3$: DMSO-d_6 = 1:1) δ: 182.8, 180.1, 167.8, 163.6, 155.0, 138.0, 132.0, 128.5, 127.8, 126.5, 119.3, 114.1, 62.1, 54.9, 51.1, 50.8, 33.0. HRESIMS m/z 392.1975 $[M + H]^+$ (calcd for $C_{23}H_{26}N_3O_3$, 392.1974).

Compound 7. Brunette powder, yield: 76.9%. ^{1}H NMR(400 MHz, $CDCl_3$: DMSO-d_6 = 1:1) δ: 9.36 (s, 1H), 7.49 (d, J = 7.8 Hz, 1H), 7.40 (s, 1H), 7.29 (d, J = 4.4 Hz, 3H), 7.22 (q, J = 4.4 Hz, 1H), 6.83 (d, J = 8.8 Hz, 1H), 6.74 (dd, J = 8.6, 2.4 Hz, 1H), 3.92 (d, J = 11.0 Hz, 1H), 3.82 (s, 3H), 3.77 (s, 3H), 3.49 (s, 2H), 2.81 (d, J = 11.4 Hz, 2H), 2.13 (t, J = 11.2 Hz, 2H), 2.04−1.92 (m, 2H), 1.59 (tt, J = 11.2, 5.8 Hz, 2H). ^{13}C- NMR (100 MHz, $CDCl_3$: DMSO-d_6 = 1:1) δ: 182.7, 180.3, 167.9, 163.4, 149.2, 144.4, 138.0, 132.7, 128.5, 127.8, 126.5, 112.1, 109.1, 103.2, 62.1, 55.7, 55.3, 51.1, 50.8, 33.0. HRESIMS m/z 422.2076 $[M + H]^+$ (calcd for $C_{24}H_{28}BrN_3O_4$, 422.2080).

Compound 8. White powder, yield: 70.4%. ^{1}H NMR(400 MHz, $CDCl_3$: DMSO-d_6 = 1:1) δ: 9.56 (s, 1H), 8.15 (s, 1H), 7.64 (s, 1H), 7.43−7.38 (m, 4H), 7.30 (d, J = 4.4 Hz, 3H), 7.23 (d, J = 4.6 Hz, 1H), 3.92 (s, 1H), 3.50 (s, 2H), 2.81 (d, J = 11.4 Hz, 2H), 2.13 (t, J = 11.2 Hz, 2H), 2.05−1.94 (m, 2H), 1.59 (d, J = 11.4 Hz, 2H). ^{13}C NMR (100 MHz, $CDCl_3$: DMSO-d_6 = 1:1) δ: 183.4, 179.9, 168.2, 162.9, 138.1, 137.9, 131.7, 128.5, 127.7, 126.5, 119.5, 114.3, 62.1, 51.1, 50.8, 32.9. HRESIMS m/z 440.0985 $[M + H]^+$ (calcd for $C_{22}H_{23}BrN_3O_2$, 440.0974).

Compound 9. White powder, yield: 47.7%. ^{1}H NMR (400 MHz, $CDCl_3$: DMSO-d_6 = 1:1) δ: 6.53−6.50 (m, 4H), 6.44 (d, J = 3.8 Hz, 5H), 6.40−6.35 (m, 1H), 3.91 (s, 2H), 2.63 (s, 2H), 1.93 (d, J = 10.8 Hz, 2H), 1.70 (t, J = 1.8 Hz, 1H), 1.35−1.21 (m, 2H), 1.08 (d, J = 12.0 Hz, 2H), 0.69 (q, J = 9.8 Hz, 2H). ^{13}C NMR (100 MHz, $CDCl_3$: DMSO-d_6 = 1:1) δ: 180.9, 180.8, 165.8, 165.5, 137.0, 136.8, 127.2, 127.1, 126.5, 126.1, 126.0, 125.3, 60.9, 49.8, 49.0, 45.6, 31.7. HRESIMS m/z 376.2023 $[M + H]^+$ (calcd for $C_{23}H_{26}N_3O_2$, 376.2025).

Compound 10. White powder, yield: 85.9%. ^{1}H NMR (400 MHz, $CDCl_3$: DMSO-d_6 = 1:1) δ: 6.35 (d, J = 5.8 Hz, 4H), 6.29 (dd, J = 6.2, 2.4 Hz, 1H), 6.20 (d, J = 8.6 Hz, 2H), 5.82 (d, J = 8.4 Hz, 2H), 3.67 (s, 2H), 2.89−2.80 (m, 1H), 1.81 (d, J = 11.2 Hz, 2H), 1.59−1.45 (m, 2H), 1.25−1.08 (m, 2H), 0.96 (d, J = 12.2 Hz, 2H), 0.58 (q, J = 11.6 Hz, 2H). ^{13}C NMR (100 MHz, $CDCl_3$: DMSO-d_6 = 1:1) δ: 180.5, 180.2, 165.3, 165.0, 155.0, 136.4, 127.2, 126.8, 126.1, 124.9, 113.4, 60.4, 49.4, 48.5, 44.7, 31.2. HRESIMS m/z 392.1975 $[M + H]^+$ (calcd for $C_{23}H_{26}N_3O_3$, 392.1974).

Compound 11. White powder, yield: 65.1%. ^{1}H NMR (400 MHz, DMSO-d_6) δ: 7.23−7.09 (m, 7H), 6.80 (d, J = 8.6 Hz, 2H), 4.51 (d, J = 6.2 Hz, 2H), 3.61 (s, 3H), 3.24 (s, 2H), 2.59 (d, J = 11.4 Hz, 2H), 2.41−2.31 (m, 1H), 1.93 (t, J = 11.2 Hz, 2H), 1.72 (s, 2H), 1.36 (q, J = 10.4, 9.8 Hz, 2H). ^{13}C NMR (100 MHz, DMSO-d_6) δ: 182.4, 182.2, 167.3, 167.2, 158.7, 138.3, 130.9, 129.1, 128.8, 128.2, 126.9, 114.1, 62.0, 55.1, 51.2, 50.5, 46.3, 33.0. HRESIMS m/z 406.2151 $[M + H]^+$ (calcd for $C_{24}H_{28}N_3O_3$, 406.2131).

Compound 12. White powder, yield: 71.4%. ^{1}H NMR(400 MHz, DMSO-d_6) δ: 7.23−7.10 (m, 5H), 6.88−6.79 (m, 2H), 6.74 (dd, J = 8.2, 2.0 Hz, 1H), 4.50 (d, J = 6.0 Hz, 2H), 3.61 (d, J = 1.8 Hz, 6H), 3.33 (s, 2H), 3.23 (s, 1H), 2.59 (d, J = 11.2 Hz, 2H), 1.93 (t, J = 11.0 Hz, 2H), 1.73 (d, J = 12.2 Hz, 2H), 1.37 (t, J = 11.8 Hz, 2H). ^{13}C NMR (100 MHz, DMSO-d_6) δ: 182.5, 182.2, 167.4, 167.2, 148.8, 148.3, 138.3, 131.2, 128.8, 128.2, 126.9, 120.0, 111.9, 111.7, 62.0, 55.6, 55.5, 51.2, 50.5, 46.7, 33.0. HRESIMS m/z 436.2259 $[M + H]^+$ (calcd for $C_{25}H_{30}N_3O_4$, 436.2236).

Compound 13. White powder, yield: 57.3%. ^{1}H NMR (400 MHz, $CDCl_3$: DMSO-d_6 = 1:1) δ: 7.27−7.24 (m, 4H), 7.20 (d, J = 8.2 Hz, 3H), 7.13 (d, J = 7.8 Hz, 2H), 4.67 (d, J = 6.2 Hz, 2H), 3.90−3.76 (m, 1H), 3.45 (s, 2H), 2.74 (d, J = 11.4 Hz, 2H), 2.29 (s, 3H), 2.09 (t, J = 11.2 Hz, 2H), 1.90 (d, J = 12.2 Hz, 2H), 1.50 (q, J = 11.0 Hz, 2H). ^{13}C NMR (100 MHz, $CDCl_3$: DMSO-d_6 = 1:1) δ: 182.3, 182.1, 167.2, 166.9, 138.0, 136.6, 135.3, 128.9, 128.5, 127.8, 127.4, 126.5, 62.1, 51.1, 50.3, 46.8, 33.0, 20.6. HRESIMS m/z 390.2176 $[M + H]^+$ (calcd for $C_{24}H_{28}N_3O_2$, 390.2182).

Compound 14. White powder, yield: 71.9%. ^{1}H NMR(400 MHz, $CDCl_3$: TFA-d = 10:1) δ: 7.66−7.57 (m, 5H), 7.52−7.43 (m, 2H), 7.28 (d, J = 8.2 Hz, 2H), 4.89 (s, 2H), 4.55−4.46 (m, 1H), 4.39 (s, 2H), 3.74 (d, J = 12.4 Hz, 2H), 3.22 (td, J = 12.6, 4.8 Hz, 2H), 2.40−2.33 (m, 4H). ^{13}C NMR (100 MHz, $CDCl_3$: TFA-d = 10:1) δ: 183.2, 182.3, 170.6, 169.1, 137.7, 135.5, 134.4, 133.7, 133.1, 132.7, 129.9, 126.0, 65.0, 54.9, 52.1, 51.5, 32.7. HRESIMS m/z 454.1126 $[M + H]^+$ (calcd for $C_{23}H_{25}BrN_3O_2$, 454.1130).

Compound 15. White powder, yield: 72.6%. ^{1}H NMR (400 MHz, Acetic Acid-d_4: DMSO-d_6 = 1:1) δ: 8.06−7.87 (m, 5H), 7.82−7.62 (m, 5H), 4.74 (s, 2H), 4.53 (s, 1H), 4.27 (t, J = 7.0 Hz, 2H), 3.88 (d, J = 12.8 Hz, 2H), 3.66−3.49 (m, 2H), 3.34 (t, J = 7.0 Hz, 2H), 3.07 (t, J = 2.2 Hz, 2H), 2.60 (d, J = 11.2 Hz, 2H). ^{13}C NMR (100 MHz, Acetic Acid-d_4: DMSO-d_6 = 1:1) δ: 188.5, 188.0, 174.3, 172.8, 144.5, 137.3, 135.7, 135.7, 135.0, 134.9, 134.5, 132.4, 65.2, 56.0, 53.9, 50.8, 43.1, 35.8. HRESIMS m/z 390.2162 $[M + H]^+$ (calcd for $C_{24}H_{28}N_3O_2$, 390.2182).

Compound 16. White powder, yield: 87.1%. ^{1}H NMR (400 MHz, $CDCl_3$: DMSO-d_6 = 1:1) δ: 9.00 (s, 1H), 7.26−7.21 (m, J = 4.0, 5H), 6.98 (d, J = 8.4 Hz, 2H), 6.68 (d, J = 8.6 Hz, 2H), 3.82 (s, 1H), 3.71 (d, J = 6.6 Hz, 2H), 3.45 (s, 2H), 2.73 (q, J = 7.8, 6.6 Hz, 4H), 2.08 (t, J = 11.2 Hz, 2H), 1.88 (d, J = 10.2 Hz, 2H), 1.48 (q, J = 12.8, 11.6 Hz, 2H). ^{13}C NMR (100 MHz, $CDCl_3$: DMSO-d_6 = 1:1) δ: 182.1, 181.8, 167.4, 166.7, 155.5, 137.8, 129.1, 128.3, 127.9, 127.6, 126.3, 114.9, 61.9, 51.0, 50.1, 44.7, 36.0, 32.8. HRESIMS m/z 406.2127 $[M + H]^+$ (calcd for $C_{24}H_{28}N_3O_3$, 406.2131).

Compound 17. White powder, yield: 76.7%. ^{1}H NMR (400 MHz, $CDCl_3$: DMSO-d_6 = 1:1) δ: 7.98 (s, 5H), 7.25 (s, 2H), 6.88 (d, J = 8.4 Hz, 2H), 6.54 (d, J = 8.2 Hz, 2H), 3.81 (s, 1H), 3.69 (t, J = 6.6 Hz, 2H), 3.44 (s, 2H), 3.29 (d, J = 9.6 Hz, 2H), 2.75 (d, J = 11.8 Hz, 2H), 2.68 (t, J = 6.8 Hz, 2H), 2.13−2.02 (m, 2H), 1.89 (d, J = 10.4 Hz, 2H), 1.48 (td, J = 10.8, 7.2 Hz, 2H). ^{13}C NMR (100 MHz, $CDCl_3$: DMSO-d_6 = 1:1) δ: 180.9, 180.6, 166.2, 165.4, 144.8, 136.7, 127.6, 127.2, 126.4, 125.2, 124.3, 112.9, 60.9, 49.8, 48.9, 43.5, 34.9, 31.7. HRESIMS m/z 405.2283 $[M + H]^+$ (calcd for $C_{24}H_{29}N_4O_2$, 405.2291).

Compound 18. White powder, yield: 79.4%. ^{1}H NMR (400 MHz, DMSO-d_6) δ: 7.36−7.19 (m, 5H), 7.11 (s, 4H), 3.85−3.64 (m, 4H), 3.47 (s, 2H), 2.78 (s, 2H), 2.73 (s, 1H), 2.25 (s,

https://doi.org/10.1021/acsomega.3c01427
ACS Omega 2023, 8, 21802−21812

3H), 2.05 (s, 2H), 1.84 (s, 2H), 1.47 (s, 2H). ^{13}C NMR (100 MHz, $CDCl_3$: TFA-*d* = 10:1) *δ*: 180.8, 180.1, 168.3, 166.1, 136.8, 133.9, 131.0, 130.9, 129.9, 129.5, 128.7, 127.4, 61.6, 51.7, 48.9, 46.4, 36.8, 29.8, 21.0. HRESIMS *m/z* 404.2348 $[M + H]^+$ (calcd for $C_{25}H_{30}N_3O_2$, 404.2338).

Compound 19. White powder, yield: 70.4%. ^{1}H NMR (400 MHz, $CDCl_3$: DMSO-d_6 = 1:1) *δ*: 6.39−6.31 (m, 4H), 6.37−6.26 (m, 2H), 5.97−5.82 (m, 3H), 2.93−2.87 (m, 1H), 2.86 (s, 3H), 2.57 (s, 2H), 1.94 (t, *J* = 7.0 Hz, 2H), 1.87 (d, *J* = 11.0 Hz, 2H), 1.63 (q, *J* = 1.8 Hz, 2H), 1.19 (t, *J* = 11.2 Hz, 2H), 1.06−0.94 (m, 2H), 0.60 (q, *J* = 10.4 Hz, 2H). ^{13}C NMR (100 MHz, $CDCl_3$: DMSO-d_6 = 1:1) *δ*: 180.8, 180.6, 166.0, 165.3, 157.7, 138.3, 136.7, 127.7, 127.1, 126.4, 125.1, 119.3, 112.7, 110.2, 60.7, 53.2, 49.7, 48.8, 42.8, 35.6, 31.6. HRESIMS *m/z* 420.2276 $[M + H]^+$ (calcd for $C_{25}H_{30}N_3O_3$, 420.2287).

Compound 20. White powder, yield: 76.9%. ^{1}H NMR (400 MHz, $CDCl_3$: DMSO-d_6 = 1:1) *δ*: 7.28 (d, *J* = 8.2 Hz, 1H), 7.24 (s, 1H), 7.23−7.19 (m, 1H), 7.00 (d, *J* = 8.2 Hz, 1H), 6.93−6.89 (m, 1H), 6.79 (d, *J* = 8.8 Hz, 1H), 6.74 (d, *J* = 1.8 Hz, 2H), 3.83 (s, 3H), 3.81 (s, 3H), 3.46 (s, 2H), 2.82 (s, 1H), 2.79−2.72 (m, 6H), 2.10 (t, *J* = 10.4 Hz, 2H), 1.94 (d, *J* = 9.2 Hz, 2H), 1.49 (q, *J* = 11.4 Hz, 2H). ^{13}C NMR (100 MHz, $CDCl_3$: DMSO-d_6 = 1:1) *δ*: 182.3, 182.1, 167.3, 166.8, 148.2, 146.9, 137.4, 130.3, 128.5, 127.5, 126.4, 120.2, 111.7, 110.8, 62.3, 55.3, 55.2, 51.1, 50.3, 44.6, 36.5, 33.0. HRESIMS *m/z* 450.2404 $[M + H]^+$ (calcd for $C_{22}H_{24}N_3O_2$, 450.2393).

Compound 21. White powder, yield: 66.5%. ^{1}H NMR(400 MHz, Acetic Acid-d_4: DMSO-d_6 = 1:1) *δ*: 8.04 (d, *J* = 3.4 Hz, 2H), 8.02−7.98 (m, 5H), 7.72 (d, *J* = 8.2 Hz, 2H), 4.82 (s, 2H), 4.59 (s, 1H), 4.32 (t, *J* = 6.8 Hz, 2H), 4.00−3.90 (m, 2H), 3.62 (dt, *J* = 12.2, 6.2 Hz, 2H), 3.39 (t, *J* = 7.0 Hz, 2H), 3.14 (t, *J* = 2.0 Hz, 2H), 2.67 (d, *J* = 13.4 Hz, 2H). ^{13}C NMR (100 MHz, Acetic Acid-d_4: DMSO-d_6 = 1:1) *δ*: 188.9, 188.4, 174.6, 173.3, 144.3, 137.7, 137.6, 137.5, 136.1, 136.0, 135.3, 126.0, 65.6, 56.3, 54.3, 50.8, 42.8, 36.1. HRESIMS *m/z* 468.1276 $[M + H]^+$ (calcd for $C_{24}H_{27}BrN_3O_2$, 468.1287).

4.2. In Vitro Anti-ChE Assay. The cholinesterase inhibitory activity of the target compounds was measured using Ellman's assay. AChE (E.C.3.1.1.7, Type VI-S, from Electric Eel), 5,5′-dithiobis (2-nitrobenzoic acid) (Ellman's reagent, DTNB), and acetylthiocholine (ATC) were purchased from Sigma-Aldrich (Steinheim, Germany). The experimental process is as follows: the compounds to be tested were diluted in DMSO to 25 and 12.5 μM and all measurements were carried out in 0.2 M NaH_2PO_4/Na_2HPO_4 buffer (pH 6.7, pH 8.0). AChE, iodothioacetylcholine (ATCI), and 5-dithiobis (2-nitrobenzoic acid) (DTNB) were all dissolved in phosphate buffer and prepared for use. The enzyme solution was prepared by dissolving 2.6 mg (0.5 U/mL) of AChE in pH 8.0 buffer (1 mL). Phosphate buffer (pH = 6.7) (140 μL 0.2 M) was added to each well in the 96-well plate. The sample solution (10 μL) and 10 μL of enzyme solution were added in the experimental group, 20 μL of phosphate buffer was added in the background control group, and 10 μL of phosphate buffer and 10 μL of enzyme solution were added in the blank control group. There are three compound holes in each group. After each hole was mixed evenly, 20 min was incubated at 25 °C. Then, DTNB (0.75 mM, 10 μL) solution and ATCI (1.5 mM, 10 μL) solution were added to incubate for 20 min at 37 °C. Then, the absorbance of each hole was detected at 405 nm wavelength and the inhibition rate was calculated. The formula for the AChE inhibition rate is as follows: AChE inhibition rate (%) = $(OD_{\text{blank control group}} - OD_{\text{test group}})/(OD_{\text{blank control group}} - OD_{\text{background control group}}) \times 100\%$.

4.3. Molecular Docking Analysis. Database and software database: (1) protein database (Protein Data Bank, referred to as PDB database, https://www.rcsb.org/) is a database for storing three-dimensional structures of macromolecules such as proteins and nucleic acids, which is created and managed by the World protein data Organization (Worldwide Protein Data Bank). (2) The structure of compound **3** was drawn in Chem Draw and copied into the SMILES format and introduced into Discovery Studio. First, all small molecules in the chemistry-hydrogen function were hydrotreated, and then, ligand preparation (Prepare Ligands) and energy minimization (Minimize Ligands) were carried out under the small molecules function module of the software. It is worth noting that the basic nitrogen atoms in compound **3** will form salt in the body. In order to simulate this situation, it is necessary to increase the charge on the nitrogen atoms. The AChE protein file was obtained from the PDB database and imported into the Discovery Studio software. The nonprotein components such as water molecules and small molecular ligands were deleted from the Hierarchy interface; then, the protein was hydrogenated under chemistry hydrogen, and then, the receptor protein was processed under the Macromolecules function module of the Discovery Studio software, and the protein was cleaned by Clean Protein function. The processed protein was saved as a PDB format file for backup. (3) Using the COCKER algorithm in Discovery Studio software, the processed receptor protein file and ligand file are set to dock the receptors and ligands needed for docking. When the ligand and receptor dock successfully in a reasonable way, it will reduce the overall energy, that is, the docking binding energy is negative, and the lower the value, the closer the binding. If the binding energy is positive, it shows that the docking is unreasonable.

4.4. Determination of Toxicity against the SH-SY5Y Cell Line. The toxicity of all compounds was determined and evaluated by the MTT method. Human SH-SY5Y neuroblastoma cells were purchased from ATCC (Manassas, VA, USA) and cultured in a wet incubator of 5% CO_2 at 37 °C, and MTT were purchased from Sigma-Aldrich (St. Louis, MO, USA). The specific steps are to dissolve the sample with DMSO and then dilute it to 12.5 μM in a medium and prepared it for use. SH-SY5Y cells were cultured overnight in 100 μL medium with a density of 8000 cells per well. After the cells were incubated with the compound for 24 h, the culture medium was removed and 0.5 mg/μL MTT was added. After incubation at 37 °C for 4 h, 150 μL of dimethyl sulfoxide (DMSO) was added to each hole and shaken slowly for 5 min. The absorbance was detected by an enzyme labeling instrument (492 nm).

4.5. Determination of Neuroprotection against the SH-SY5Y Cell Line. The neuroprotective activities of all compounds in human SH-SY5Y cell lines were measured and evaluated by the MTT method. The specific steps were that the sample was dissolved in DMSO and diluted to 12.5 μM in the medium for use. SH-SY5Y cells were inoculated overnight in 100 μL medium with a density of 8000 cells per well. After the cells were incubated with the compound for 24 h, the culture medium was removed, and hydrogen peroxide solution (H_2O_2 650 μM) was added to the cells, incubated for 4 h, and 0.5 mg/μL MTT was added. After incubation at 37 °C for 4 h, 150 μL of dimethyl sulfoxide (DMSO) was added to each hole and 10 min was shaken on the shaker. The absorbance value was detected by an enzyme labeling instrument (492 nm). The cell survival rate was

https://doi.org/10.1021/acsomega.3c01427
ACS Omega 2023, 8, 21802−21812

calculated as follows: cell inhibition rate (%) = 1 − ($OD_{test\ group}$ − $OD_{blank\ group}$/$OD_{control\ group}$ − $OD_{blank\ group}$) × 100%.

4.6. Reactive Oxygen Species for Flow Cytometric Analysis. Reactive oxygen species (ROS) for flow cytometry analysis. SH-SY5Y cells (9 × 105 cells/mL) are cultured in 6-well plates for 24 h and then pretreated with compound **3** (12.5 μM). After 24 h of incubation, the cells are collected and centrifuged after treating them with hydrogen peroxide solution (H_2O_2, 850 μM). Then, DCFH-DA is added to stain the ROS in the cells for 30 min at 37 °C. The stained cells were collected and analyzed using the FACS Caliber instrument (Becton Dickinson, Mountain View, California, USA).

4.7. Immunofluorescence. After incubating SH-SY5Y cells (8 × 104 cells/mL) in a 24-well plate for 24 h, compound **3** (12.5 μM) is added overnight. Hydrogen peroxide solution (H_2O_2, 850 μM) is subsequently added and incubated for another 4 h. The supernatant is aspirated and the exposed cells are fixed with 4% paraformaldehyde for 30 min. After three washes with PBS, the cells are treated with 0.2% TritonX-100 for 5 min. Subsequently, apoptotic cells were detected using the Tunel Apoptosis Assay Kit (Beyotime Institute of Biotechnology, Shanghai, China) and observed under a fluorescence microscope.

4.8. ADMET Analysis. The "pkCSM-pharmacokinetics" online platform was used for the prediction of the pharmacokinetics of compound **3** by analyzing parameters of lipophilicity, water solubility, pharmacokinetics, and druglikeness. The 2D structure of compound **3** was drawn in the ChemBioDraw Ultra 13.0 software and then converted to the SMILE sequence. Then, the SMILE was uploaded in the pkCSM online server (http://www.swissadme.ch/) in order to obtain the predicted pharmacokinetics profile of compound **3**.

4.9. Evaluation of the Complexing Ability of Metal Ions. Chelation was studied by UV−vis spectroscopy. The UV absorption spectra of compound **3** were determined after one hour of incubation at room temperature, both individually and in the presence of $CuCl_2$, $ZnCl_2$, $AlCl_3$, and $FeSO_4$.The wavelength range is 190∼400 nm. The final volume of the reaction mixture is 3 mL, and the final concentration of the tested compound and metal is 35.0 μM.

■ ASSOCIATED CONTENT

Supporting Information

The Supporting Information is available free of charge at https://pubs.acs.org/doi/10.1021/acsomega.3c01427.

^{1}H and ^{13}C NMR spectra for all the new compounds (PDF)

■ AUTHOR INFORMATION

Corresponding Authors

Lin Chen − *School of Life Science and Engineering, Southwest Jiaotong University, Chengdu 610031 Sichuan, P.R. China;* orcid.org/0000-0001-5423-4708; Email: linch@swjtu.edu.cn; Fax: +86-28-66367260

Xian-Li Zhou − *School of Life Science and Engineering, Southwest Jiaotong University, Chengdu 610031 Sichuan, P.R. China; Affiliated Hospital of Southwest Jiaotong University & The Third People Hospital of Chengdu, Chengdu 610031 Sichuan, P.R. China;* orcid.org/0000-0002-1690-0578; Email: zhouxl@swjtu.edu.cn; Fax: +86-28-66367260

Authors

Dan Wan − *School of Life Science and Engineering, Southwest Jiaotong University, Chengdu 610031 Sichuan, P.R. China*

Feng-Qin Wang − *School of Life Science and Engineering, Southwest Jiaotong University, Chengdu 610031 Sichuan, P.R. China*

Jiang Xie − *Affiliated Hospital of Southwest Jiaotong University & The Third People Hospital of Chengdu, Chengdu 610031 Sichuan, P.R. China*

Complete contact information is available at: https://pubs.acs.org/10.1021/acsomega.3c01427

Notes

The authors declare no competing financial interest.

■ ACKNOWLEDGMENTS

This work was financially supported by the Research Foundation for Administration of Traditional Chinese Medicine of Sichuan Province (2020HJZX002), the Fundamental Research Funds for the Central Universities (2682023ZTPY051), and the National Natural Science Foundation of China (82073734).

■ REFERENCES

(1) Chen, Y.; Bian, Y.-M.; Wang, J.-W.; Gong, T.-T.; Ying, Y.-M.; Ma, L.-F.; Shan, W.-G.; Xie, X.-Q.; Zhan, Z.-J. Effects of α-Mangostin Derivatives on the Alzheimer's Disease Model of Rats and Their Mechanism: A Combination of Experimental Study and Computational Systems Pharmacology Analysis. *ACS Omega* **2020**, *5*, 9846−9863.

(2) Wan, L.-X.; Miao, S.-X.; He, Z.-X.; Li, X.-H.; Zhou, X.-L.; Gao, F. Pd-Catalyzed Direct Modification of an Anti-Alzheimer's Disease Drug: Synthesis and Biological Evaluation of alpha-Aryl DNP Analogues. *ACS Omega* **2021**, *6*, 23347−23354.

(3) Kareem, R. T.; Abedinifar, F.; Mahmood, E. A.; Ebadi, A. G.; Rajabi, F.; Vessally, E. The recent development of donepezil structure-based hybrids as potential multifunctional anti-Alzheimer's agents: highlights from 2010 to 2020. *RSC Adv.* **2021**, *11*, 30781−30797.

(4) Singh, J. V.; Thakur, S.; Kumar, N.; Singh, H.; Mithu, V. S.; Singh, H.; Bhagat, K.; Gulati, H. K.; Sharma, A.; Singh, H.; Sharma, S.; Bedi, P. M. S. Donepezil-Inspired Multitargeting Indanone Derivatives as Effective Anti-Alzheimer's Agents. *ACS Chem. Neurosci.* **2022**, *13*, 733−750.

(5) Brunetti, L.; Leuci, R.; Carrieri, A.; Catto, M.; Occhineri, S.; Vinci, G.; Gambacorta, L.; Baltrukevich, H.; Chaves, S.; Laghezza, A.; Altomare, C. D.; Tortorella, P.; Santos, M. A.; Loiodice, F.; Piemontese, L. Structure-based design of novel donepezil-like hybrids for a multi-target approach to the therapy of Alzheimer's disease. *Eur. J. Med. Chem.* **2022**, *237*, No. 114358.

(6) Li, Q.; He, S.-Y.; Chen, Y.; Feng, F.; Qu, W.; Sun, H. Donepezil-based multi-functional cholinesterase inhibitors for treatment of Alzheimer's disease. *Eur. J. Med. Chem.* **2018**, *158*, 463−477.

(7) Unsal-Tan, O.; Ozadali-Sari, K.; Ayazgok, B.; Kucukkilinc, T. T.; Balkan, A. Novel 2-Arylbenzimidazole derivatives as multi-targeting agents to treat Alzheimer's disease. *Med. Chem. Res.* **2017**, *26*, 1506−1515.

(8) Choubey, P. K.; Tripathi, A.; Sharma, P.; Shrivastava, S. K. Design, synthesis, and multitargeted profiling of N-benzylpyrrolidine derivatives for the treatment of Alzheimer's disease. *Bioorg. Med. Chem.* **2020**, *28*, No. 115721.

(9) Yang, G.-X.; Huang, Y.; Zheng, L.-L.; Zhang, L.; Su, L.; Wu, Y.-H.; Li, J.; Zhou, L.-C.; Huang, J.; Tang, Y.; Wang, R.; Ma, L. Design, synthesis and evaluation of diosgenin carbamate derivatives as multitarget anti-Alzheimer's disease agents. *Eur. J. Med. Chem.* **2020**, *187*, No. 111913.

(10) Cheignon, C.; Tomas, M.; Bonnefontrousselot, D.; Faller, P.; Hureau, C.; Collin, F. Oxidative stress and the amyloid beta peptide in alzheimer's disease. *Redox Biol.* **2018**, *14*, 450−464.
(11) Bosquesi, P. L.; Melo, T. R. F.; Vizioli, E. O.; Santos, J. L.; Chung, M. C. Anti-Inflammatory Drug Design Using a Molecular Hybridization Approach. *Pharmaceuticals* **2011**, *4*, 1450−1474.
(12) Gontijo, V. S.; Viegas, F. P. D.; Ortiz, C. J. C.; Silva, M. D. F.; Damasio, C. M.; Rosa, M. C.; Campos, T. G.; Couto, D. S.; Dias, K. S. T.; Viegas, C. Molecular Hybridization as a Tool in the Design of Multitarget Directed Drug Candidates for Neurodegenerative Diseases. *Curr. Neuropharmacol.* **2020**, *18*, 348−407.
(13) Benek, O.; Korabecny, J.; Soukup, O. A Perspective on Multitarget Drugs for Alzheimer's Disease. *Trends Pharmacol. Sci.* **2020**, *41*, 434.
(14) Teng, L.-B.; Qian, J. Progress in the synthesis of benoxate. *Shandong Chem. Ind.* **2009**, *8*, 3 DOI: 10.3969/j.issn.1008-021X.2009.08.008.
(15) Silva, M. A.; Kiametis, A. S.; Treptow, W. Donepezil inhibits acetylcholinesterase via multiple binding modes at room temperature. *J. Chem. Inf. Model.* **2020**, *60*, 3463−3471.
(16) Prati, F.; Cavalli, A.; Bolognesi, M. L. Navigating the chemical space of multitarget-directed ligands: from hybrids to fragments in Alzheimer's disease. *Molecules* **2016**, *21*, 466.
(17) Wang, Z. M.; Cai, P.; Liu, Q. H.; Xu, D. Q.; Yang, X. L.; Wu, J. J.; Kong, L. Y.; Wang, X. B. Rational modification of donepezil as multifunctional acetylcholinesterase inhibitors for the treatment of alzheimer's disease. *Eur. J. Med. Chem.* **2016**, *123*, 282−297.
(18) Asakawa, D.; Mizuno, H.; Sugiyama, E.; Todoroki, K. In-source fragmentation of phenethylamines by electrospray ionization mass spectrometry: toward highly sensitive quantitative analysis of monoamine neurotransmitters. *Anal. Chem.* **2020**, *92*, 12033−12039.
(19) Svobodova, B.; Mezeiova, E.; Hepnarova, V.; Hrabinova, M.; Korabecny, J. Exploring structure-activity relationship in tacrine-squaramide derivatives as potent cholinesterase inhibitors. *Biomolecules* **2019**, *9*, 379.
(20) Chauhan, P.; Mahajan, S.; Kaya, U.; Hack, D.; Enders, D. Bifunctional amine-squaramides: powerful hydrogen-bonding organocatalysts for asymmetric domino/cascade reactions. *Adv. Synth. Catal.* **2015**, *357*, 253−281.
(21) Nikolova, Y.; Dobrikov, G.; Petkova, Z.; Shestakova, P. Chiral aminoalcohols and squaric acid amides as ligands for asymmetric borane reduction of ketones: insight to in situ formed catalytic system by DOSY and multinuclear NMR experiments. *Molecules* **2021**, *26*, 6865.
(22) Ellman, G. L.; Courtney, K. D.; Andres, V., Jr.; Featherstone, R. M. A new and rapid colorimetric determination of acetylcholinesterase activity. *Biochem. Pharmacol.* **1961**, *7*, 88−95.
(23) Niyazi, H.; Hall, J. P.; O″Sullivan, K.; Winter, G.; Sorensen, T.; Kelly, J. M.; Cardin, C. J. Crystal structures of lambda-[Ru(phen)-2dppz]2+ with oligonucleotides containing TA/TA and AT/AT steps show two intercalation modes. *Nat. Chem.* **2012**, *4*, 621−628.
(24) Brown, E.; Markman, M. Tumor chemosensitivity and chemoresistance assays. *Cancer* **1996**, *77*, 1020−1025.
(25) Putnam, C. D.; Arvai, A. S.; Bourne, Y.; Tainer, J. A. Active and inhibited human catalase structures: ligand and NADPH binding and catalytic mechanism. *J. Mol. Biol.* **2000**, *296*, 295−309.
(26) Tönnies, E.; Trushina, E. Oxidative stress, synaptic dysfunction, and alzheimer's disease. *J. Alzheimer's Dis.* **2017**, *57*, 1105−1121.
(27) Wang, L.; Yin, Y. L.; Liu, X. Z.; Shen, P.; Wang, J. Z. Current understanding of metal ions in the pathogenesis of alzheimer's disease. *Transl. Neurodegener.* **2020**, *9*, 10.
(28) Cai, R.; Wang, L. N.; Fan, J. J.; Geng, S. Q.; Liu, Y. M. New 4-n-phenylaminoquinoline derivatives as antioxidant, metal chelating and cholinesterase inhibitors for alzheimer's disease. *Bioorg. Chem.* **2019**, *93*, No. 103328.

https://doi.org/10.1021/acsomega.3c01427
ACS Omega 2023, 8, 21802−21812